



OPEN ACCESS

EDITED BY

Tom Millar,
Queen's University Belfast, United Kingdom

REVIEWED BY

Xuan Fang,
Chinese Academy of Sciences (CAS), China
Schmidt Schmidt,
Polish Academy of Sciences, Poland

*CORRESPONDENCE

Xiaofeng Yang,
✉ xfyang@xao.ac.cn

RECEIVED 11 May 2024

ACCEPTED 27 May 2024

PUBLISHED 25 June 2024

CITATION

Yang J, Yang X and Zhu C (2024), A deep search for C₂H in the oxygen-rich post-AGB star OH 231.8+4.2.
Front. Astron. Space Sci. 11:1431250.
doi: 10.3389/fspas.2024.1431250

COPYRIGHT

© 2024 Yang, Yang and Zhu. This is an open-access article distributed under the terms of the [Creative Commons Attribution License \(CC BY\)](https://creativecommons.org/licenses/by/4.0/). The use, distribution or reproduction in other forums is permitted, provided the original author(s) and the copyright owner(s) are credited and that the original publication in this journal is cited, in accordance with accepted academic practice. No use, distribution or reproduction is permitted which does not comply with these terms.

A deep search for C₂H in the oxygen-rich post-AGB star OH 231.8+4.2

Jianchao Yang^{1,2}, Xiaofeng Yang^{1,3*} and Cheng Zhu^{1,4}

¹Xinjiang Astronomical Observatory, Chinese Academy of Sciences, Urumqi, China, ²University of Chinese Academy of Sciences, Beijing, China, ³Xinjiang Key Laboratory of Radio Astrophysics, Urumqi, China, ⁴Beijing National Laboratory for Molecular Sciences (BNLMS), Institute of Chemistry, Chinese Academy of Sciences, Beijing, China

In carbon-rich environment, C₂H emission is seen to be associated with HC₃N, but whether it can trace the HC₃N molecule in oxygen-rich environment is unknown. Here, we have searched for rotational emission from ethynyl radical (C₂H) in the oxygen-rich circumstellar envelope (CSE) of the post-asymptotic giant branch (post-AGB) star OH 231.8+4.2, a renowned galactic proto-planetary nebula (PPN) known to display cyanoacetylene (HC₃N) emission. Our observations were conducted using the James Clerk Maxwell Telescope (JCMT), and the total on-source time is 11.9 h. Base on local thermodynamic equilibrium (LTE) excitation analysis, we have calculated the column density and the abundance relative to H₂ for C₂H. The calculated column density for C₂H is less than $1.4 \times 10^{13} \text{ cm}^{-2}$, which corresponds to a fractional abundance, $f(\text{C}_2\text{H})$, less than 4.5×10^{-9} . This inference suggests that the typical transformation pathway from C₂H and C₂H₂ to HC₃N may not play a significant role in O-rich environments. It indicates the presence of alternative, unidentified pathways that contribute to the formation of HC₃N in O-rich circumstellar envelopes.

KEYWORDS

post-AGB star, circumstellar envelopes (CSEs), column density, C₂H, OH 231.8+4.2

1 Introduction

The post-asymptotic giant branch (post-AGB) star, or proto-planetary nebula (PPN), OH 231.8+4.2, has been extensively studied on account of its unusual chemistry (Sánchez Contreras et al., 1997). This complex object exhibits a massive bipolar outflow and a rotating disk (Sánchez Contreras et al., 2022). The central star, named QX Pup, is accompanied by a binary companion star of type A0 V, indirectly identified through the analysis of the stellar spectrum reflected by the nebular dust (Sánchez Contreras et al., 2004). OH 231.8+4.2 features an oxygen-rich (O-rich) circumstellar envelope (CSE) surrounding an evolved intermediate-mass star. In addition to typical oxygen-containing species, a variety of detected ions including HCO⁺, H¹³CO⁺, SO⁺, N₂H⁺, and H₃O⁺ have been observed (Sánchez Contreras et al., 2015). Furthermore, chloride species like NaCl and KCl, as well as carbon-containing species such as HCN and HNC, were identified (Sánchez Contreras et al., 1997; Sánchez Contreras et al., 2022). CSEs are categorized based on their carbon to oxygen abundance ratio ([C]/[O]). If the [C]/[O] > 1, they are considered carbon-rich AGB stars (C-rich), while if it is < 1, they are classified as O-rich AGB stars (objects with [C]/[O] ~ 1 are known as S-type AGB stars). The chemical composition of CSEs is greatly influenced by the relative abundances of carbon and oxygen (Velilla Prieto et al., 2015). In O-rich CSEs, carbon often acts as the limiting reactant and is primarily converted

into carbon monoxide (CO), a highly abundant and stable molecule. The remaining oxygen can then combine with other elements to form additional oxygen-bearing molecules. Consequently, O-rich envelopes typically exhibit lower abundances of carbon-bearing molecules aside from CO, whereas C-rich CSEs tend to show limited amounts of oxygen-bearing species (Bujarrabal et al., 1994).

However, Velilla Prieto et al. (2015) detected HC₃N molecule for the first time in OH 231.8+4.2, which also represents the first observation of HC₃N in an oxygen-rich CSE. For linear carbon chain molecules, Agúndez et al. (2017) investigated their formation in the C-rich AGB star IRC+10216 utilizing a combined approach of observations and modeling. Their study suggests that the dissociation of acetylene (C₂H₂) and hydrogen cyanide (HCN) induced by ultraviolet photons can drive the production of steadily increasing length of linear carbon chains. In the outer regions of stars, C₂H₂ and HCN are photodissociated, producing radicals C₂H and CN, which can drive the formation of carbon chain molecules (Huggins and Glassgold, 1982; Cherchneff et al., 1993; Li et al., 2014; Agúndez et al., 2017). In carbon-rich environments, C₂H is often used to “trace” linear carbon chain molecules. Therefore, to explore the carbon chemistry mechanism in OH 231.8+4.2, We reached for C₂H emission using the James Clerk Maxwell Telescope (JCMT).

In this paper, we report the upper limits of the column density of C₂H and the abundance of C₂H relative to H₂ in the post-AGB star OH 231.8+4.2.

2 Observations and data reduction

The observations were conducted using the JCMT 15 m at Maunakea, Hawaii, from 2021 to 2023. This work used about 11.9 h (on-source) of integration on project E21AZ002 and M23BP059. We used the Namakanui instrument within 230 GHz ‘U’ü receiver. The central frequency we observed was 262.0042266 GHz. The observations were carried out in beam-switch mode and performed towards the center of OH 231.8+4.2 (RA (2000) = 07:42:16.947, Dec (2000) = -14:42:50.20). The local standard of rest (LSR) velocity of this source is 34 km s⁻¹ (Alcolea et al., 2001). We obtained pipeline-processed data by first utilizing the Starlink¹ software package ORAC-DR, and then converting the spectra to the CLASS format. Following this, we performed additional data reduction using the GILDAS² software including CLASS. The conversion of antenna temperature T_A^* to the main-beam temperature T_{mb} , was made in accordance with $T_{mb} = T_A^* / \eta_{mb}$, where the main-beam efficiency, $\eta_{mb} = 0.66$ in this band. The full width at half maximum (FWHM) of is 18.62'' at this frequency. We used a velocity resolution of 0.559 km s⁻¹. Observations were made under Band 3 (0.08 < τ < 0.12) and Band 4 (0.12 < τ < 0.2) weather conditions. We smoothed the spectra in the velocity range of -100 to 100 km ss⁻¹ (combined channels). The rms noise of the smoothed spectra is about 1 mK in 2.235 km s⁻¹ wide channels. Our data reduction results in high-quality spectra with a low noise level, allowing us to accurately analyze the observed molecular emission. All spectra have been

calibrated based on the antenna temperature (T_A^*) scale, which is inextricably linked to the average brightness temperature of the source (T_B) by the following equation, $T_B = T_{mb} / \delta$. where δ is the beam-filling factor, see Eq. 1.

In the present study, we have considered the molecular outflow emanating from OH 231.8+4.2 as a homogenous elliptical source, characterized by its major and minor axes θ_a and θ_b . Under this assumption, the beam-filling factor can be expressed as follows:

$$\delta = 1 - e^{-\ln 2 \frac{\theta_a \times \theta_b}{FWHM^2}}. \quad (1)$$

where the FWHM is Full Width at Half Maximum of the obtained beam. We adopt an angular source size of $\theta_a \times \theta_b = 4'' \times 12''$ (Morris et al., 1987). The beam filling factor in this study is 0.09.

3 Results and analysis

The lower panel of Figure 1 shows the JCMT spectrum with a center frequency of 262004.2266 MHz and a bandwidth of 1 GHz, while the upper panel displays an expanded view of the spectrum between -100 and 100 km s⁻¹. In the lower panel spectrum, we detect lines arising from SO ($J = 7_6-6_5$) and SO₂ ($J = 4_{(4,0)} - 5_{(3,3)}, J = 11_{(3,9)} - 11_{(2,10)}$). Note that their shape fits quite well to those of ¹³CO transitions on Figure 2 of Velilla Priet et al. (2015), including even some of the minor spectral features identified. However, not much can be seen as far as the shape of HC₃N transitions are concerned. In the upper panel, we mark the line positions of the $J = 7/2-5/2$ and $J = 5/2-3/2$ transitions in the $N = 3-2$ rotational transition of C₂H. In our observations the hyperfine transitions of both rotational lines ($N = 3-2, J = 7/2-5/2, F = 4-3$ (262004.2266 MHz) and $F = 3-2$ (262006.40340 MHz) and $N = 3-2, J = 5/2-3/2, F = 4-3$ (262064.8433 MHz) and $F = 2-1$ (262006.40340 MHz)) could be resolved with the original resolution, however, even if detected cannot be resolved after resampling. Despite the undertaken observational efforts, the emission of C₂H is not detected at a noise level of 1 mK. Table 1 summarizes the upper limits for the C₂H lines in OH 231.8+4.2.

To determine the column density and fractional abundance with relative to H₂, we assume that the spectral line is optically thin and all levels involved in the transitions are under local thermodynamic equilibrium (LTE) conditions. We use the rotational diagram method (see Eq. 2) to estimate the abundance of C₂H. This method has been extensively described and discussed by Goldsmith and Langer. (1999). The equation is as follows:

$$\ln\left(\frac{3kW}{8\pi^3\nu S\mu^2}\right) = \ln\left(\frac{N}{Q}\right) - \frac{E_u}{kT_{ex}}. \quad (2)$$

Here, N is the total column density of the molecule, Q is the partition function, E_u is the upper-level energy, T_{ex} is the excitation temperature, k is the Boltzmann constant, ν is the rest frequency, W ($\int T_B dv$) spectral line integral intensity, $S\mu^2$ is the product of the line strength and the square of the electric dipole moment. The values of $S\mu^2$ and $\frac{E_u}{k}$ are taken from the splatalogue databases³.

1 <http://www.starlink.ac.uk>

2 <http://www.iram.fr/IRAMFR/GILDAS>

3 <https://splatalogue.online/advanced.php>

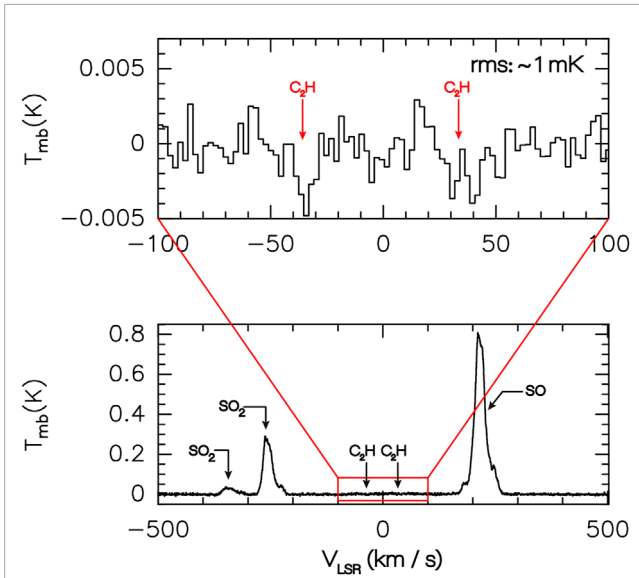


FIGURE 1 Molecular spectra observed toward OH 231.8+4.2 identified with the JCMT 15 m. The lower panel spectrum with a center frequency of 262004.2266 MHz and a bandwidth of 1 GHz, including two emission lines for SO₂ and one emission line for SO; The top panel spectrum shows frequency positions of the $J = 7/2-5/2$ and $J = 5/2-3/2$ transitions in the $N = 3-2$ rotational transition of C₂H, the root mean square (rms) noise level is 1 mK.

We assume that the excitation temperature and linewidth of C₂H are the same as HC₃N reported by Velilla Prieto et al. (2015), which are 17 K and 27 km s⁻¹. Based on our calculations, the column density of C₂H is less than 1.4×10^{13} cm⁻² (3σ upper limit).

In order to determine the relative abundance of C₂H to H₂, it is necessary to evaluate the average H₂ column density within the radius occupied by C₂H. This can be achieved by employing the following equation (Gong et al., 2015).

$$N_{H_2} = \frac{\dot{M}R/V_{exp}}{\pi R^2 m_{H_2}} = \frac{\dot{M}}{\pi R V_{exp} \mu m_H} \quad (3)$$

Here, \dot{M} is the mass-loss rate of the star; R is the radius of C₂H molecule distribution in CSE of AGB star; V_{exp} the expansion velocity; m_H the mass of hydrogen atom; $\mu = 2.8$ is the mean molecular weight. The mass loss rate of OH 231.8+4.2 is $10^{-4} M_\odot \text{ yr}^{-1}$ (Alcolea et al., 2001). The expansion velocity of this source is 20 km s⁻¹ (Sánchez Contreras et al., 1997).

Due to the lack of mapping observations on C₂H in this source, it is hypothesized that the C₂H molecule originates from the slow-moving central component of the molecular outflow that emanates from OH 231.8+4.2. The outer radius of this PPN is 7×10^{16} cm ($3''$ at $d = 1500$ pc) (Velilla Prieto et al., 2015). Following the Eq. 3 and using the upper limit of column density of C₂H, we can get that relative abundance of C₂H to H₂ is then less than 4.5×10^{-9} .

4 Discussion

In carbon-rich environment, HC₃N is formed demanding the presence of CN and C₂H₂ as parent molecules. Since C₂H₂ cannot be observed in radio wavelengths and C₂H is a result of C₂H₂ photodissociation, we have decided to search for the C₂H transitions in OH 231.8+4.2. Molecular C₂H are often used to explain the formation of HC₃N, such as in the case of PPNe CRL 618, CRL 2688, where both C₂H and HC₃N molecules have been detected (Pardo et al., 2005; Zhang et al., 2013) and which are in the same evolutionary stage as OH 231.8+4.2. Unlike CRL 618 and CRL 2688, OH 231.8+4.2 exhibits a massive bipolar outflow and a rotating disk (Sánchez Contreras et al., 2022). This leads to the presence of a diverse array of species within this source, including ions and carbon-containing species (Sánchez Contreras et al., 1997; Sánchez Contreras et al., 2015). The observed relative abundance of C₂H is higher than that of HC₃N in C-rich environments of evolved stars. For example, in IRC+10216, the relative abundances of C₂H and HC₃N are 2.8×10^{-6} and 1.25×10^{-6} ; in CRL 2688, the values of these two species are 1.22×10^{-6} and 3.83×10^{-7} , respectively, see Zhang et al. (2013). Astrochemical model also gives the same conclusion, see Li et al. (2014). However, in OH 231.8+4.2, we obtained an upper limit of 4.5×10^{-9} for C₂H fractional abundance, which is lower than the observed HC₃N abundance (7.9×10^{-9}). It is possible that the chemical environment of OH 231.8+4.2 is different from that of CRL 618 and CRL 2688. As OH 231.8+4.2 is an oxygen-rich PPN containing a large amount of oxygen atoms and hydroxyl radicals, reactions involving C₂H and oxygen atoms or OH radicals occur very quickly (Bosman et al., 2021). This results in the depletion of C₂H in OH 231.8+4.2. The presence of high-speed jets and shocks in OH 231.8+4.2 (Morris et al., 1987) may also result in unknown reactions depleting the C₂H. However, in this case HC₃N can also be significantly destroyed, so we cannot argue that this is a fully valid argument. It is also possible that C₂H₂ may not be present in sufficient abundance to form abundant C₂H through photodissociation. Hence the lack of detection of C₂H in this source is still elusive. We plan to further search for the C₂H and HC₃N

TABLE 1 Correlation parameters of C₂H observed in OH 231.8+4.2.

Species	Transition	ν	T_{mb}	rms	$\int T_{mb} dv$
		(MHz)	(mK)	(mK)	(K km s ⁻¹)
C ₂ H	$N = 3-2, J = 7/2-5/2$	262004.2266	1.20	1.20	< 0.032
C ₂ H	$N = 3-2, J = 5/2-3/2$	262064.8433	1.20	1.20	< 0.032

Note. The table includes: 1) name of the Species; 2) rotational quantum numbers; 3) rest frequency; 4) main-beam peak temperature; 5) root mean square; 6) main-beam peak temperature integrated over velocity.

in other oxygen-rich proto-planetary nebulae in the galaxy to study carbon chemistry in oxygen-rich environment.

5 Conclusion

Despite a sensitive search to a noise level of 1 mK, we did not detect emission from C₂H in OH 231.8+4.2. This result is surprising given the close correspondence between C₂H and HC₃N seen in C-rich AGB stars and the fact that in these objects, the acetylene molecule, C₂H₂, is thought to be a direct chemical precursor through its reaction with CN. Its non-detection may be due to one or more of several factors: one, that the C₂H is removed very rapidly in the oxygen-rich environment of OH 231.8+4.2; two, that the intrinsic physical properties (shocks, jets) prevent its existence; three, that C₂H₂ may not be present in sufficient abundance to form abundant C₂H through photodissociation. In this case, the HC₃N detected in OH 231.8+4.2 must be formed via a different chemical route than that which occurs in C-rich AGB circumstellar envelopes. Our study indicates the need for future research on the formation and evolution of carbon chain molecules in oxygen-rich environment.

Data availability statement

The raw data supporting the conclusion of this article will be made available by the authors, without undue reservation.

Author contributions

JY: Writing—original draft, Writing—review and editing. XY: Funding acquisition, Investigation, Resources, Writing—review and editing. CZ: Investigation, Methodology, Writing—review and editing.

References

- Agúndez, M., Cernicharo, J., Quintana-Lacaci, G., Castro-Carrizo, A., Velilla Prieto, L., Marcelino, N., et al. (2017). Growth of carbon chains in IRC+10216 mapped with ALMA. *Astronomy Astrophysics* 601, A4. doi:10.1051/0004-6361/201630274
- Alcolea, J., Bujarrabal, V., Sánchez Contreras, C., Neri, R., and Zweigle, J. (2001). The highly collimated bipolar outflow of OH 231.8+4.2. *Astronomy Astrophysics* 373 (3), 932–949. doi:10.1051/0004-6361:20010535
- Bosman, A. D., Alarcón, F., Zhang, K., and Bergin, E. A. (2021). Destruction of refractory carbon grains drives the final stage of protoplanetary disk chemistry. *Astrophysical J.* 910, 3. doi:10.3847/1538-4357/abe127
- Bujarrabal, V., Fuente, A., and Omont, A. (1994). Molecular observations of O-rich and C-rich circumstellar envelopes. *Astronomy Astrophysics* 285 (1), 247–271.
- Cherchneff, I., Glassgold, A. E., and Mamon, G. A. (1993). The Formation of cyanopolyne molecules in IRC+10216. *Astrophysical J.* 410 (1), 188–201. doi:10.1086/172737
- Goldsmith, P. F., and Langer, W. D. (1999). Population diagram analysis of molecular line emission. *Astrophysical J.* 517, 209–225. doi:10.1086/307195
- Gong, Y., Henkel, C., Spezzano, S., Thorwirth, S., Menten, K. M., Wyrowski, F., et al. (2015). A 1.3 cm line survey toward IRC+10216. *Astronomy Astrophysics* 574, A56. doi:10.1051/0004-6361/201424819
- Huggins, P. J., and Glassgold, A. E. (1982). The photochemistry of carbon-rich circumstellar shells. *Astrophysical J.* 252 (1), 201–207. doi:10.1086/159547
- Lí, X., Millar, T. J., Walsh, C., Heays, A. N., and van Dishoeck, E. F. (2014). Photodissociation and chemistry of N₂ in the circumstellar envelope of carbon-rich AGB stars. *Astronomy Astrophysics* 568, A111. doi:10.1051/0004-6361/201424076
- Morris, M., Guilloteau, S., Lucas, R., and Omont, A. (1987). The rich molecular-spectrum and the rapid outflow of OH 231.8+4.2. *Astrophysical J.* 321 (2), 888–897. doi:10.1086/165681
- Pardo, J. R., Cernicharo, J. R., Goicoechea, J. R., Guélin, M., and Phillips, T. G. (2005). The millimeter and submillimeter spectrum of CRL618. *Proc. Dusty Mol. Universe A Prelude Herschel Alma* 577, 455–456.
- Sánchez Contreras, C., Alcolea, J., Rodríguez-Cardoso, R., Bujarrabal, V., Castro-Carrizo, A., Velilla-Prieto, L., et al. (2022). ALMA (finally!) discloses a rotating disk+bipolar wind system at the centre of the wind-prominent pPN OH 231.8+4.2. *Proc. Int. Astronomical Union* 16 (S366), 301–307. doi:10.1017/s1743921322000102
- Sánchez Contreras, C., Bujarrabal, V., and Alcolea, J. (1997). The rich molecular content of OH 231.8+4.2. *Astronomy Astrophysics* 327 (2), 689–698.
- Sánchez Contreras, C., de Paz, A. G., and Sahai, R. (2004). The companion to the central mira star of the protoplanetary nebula OH 231.8+4.2. *Astrophysical J.* 616 (1), 519–524. doi:10.1086/424827
- Sánchez Contreras, C., Velilla Prieto, L., Agúndez, M., Cernicharo, J., Quintana-Lacaci, G., Bujarrabal, V., et al. (2015). Molecular ions in the O-rich evolved star OH231.8+4.2: HCO⁺, H¹³CO⁺ and first detection of SO⁺, N₂H⁺, and H₃O⁺. *Astronomy Astrophysics* 577, A52. doi:10.1051/0004-6361/201525652
- Velilla Prieto, L., Sánchez Contreras, C., Cernicharo, J., Agúndez, M., Quintana-Lacaci, G., Alcolea, J., et al. (2015). New N-bearing species towards OH 231.8+4.2. *Astronomy Astrophysics* 575, A84. doi:10.1051/0004-6361/201424768
- Zhang, Y., Kwok, S., Nakashima, J.-i., Chau, W., and Dinh, V. T. (2013). A molecular line survey of the carbon-rich protoplanetary nebula AFGL 2688 in the 3 mm and 1.3 mm windows. *Astrophysical J.* 773, 71. doi:10.1088/0004-637x/773/1/71

Funding

The author(s) declare that financial support was received for the research, authorship, and/or publication of this article. CZ thanks the Xinjiang Tianchi Talent Program (2024). This work is supported by the National SKA Program of China No. 2022SKA0110203 and Xiaofeng Yang's CAS Pioneer Hundred Talents Program. The James Clerk Maxwell Telescope is operated by the East Asian Observatory on behalf of The National Astronomical Observatory of Japan; Academia Sinica Institute of Astronomy and Astrophysics; the Korea Astronomy and Space Science Institute; the National Astronomical Research Institute of Thailand; Center for Astronomical Mega-Science (as well as the National Key R&D Program of China with No. 2017YFA0402700); Additional funding support is provided by the Science and Technology Facilities Council of the United Kingdom and participating universities and organizations in the United Kingdom and Canada. This work was supported by the JCMT E21AZ002 and M23BP059 project.

Conflict of interest

The authors declare that the research was conducted in the absence of any commercial or financial relationships that could be construed as a potential conflict of interest.

Publisher's note

All claims expressed in this article are solely those of the authors and do not necessarily represent those of their affiliated organizations, or those of the publisher, the editors and the reviewers. Any product that may be evaluated in this article, or claim that may be made by its manufacturer, is not guaranteed or endorsed by the publisher.